ISSN 1068-7998, Russian Aeronautics (Iz.VUZ), 2018, Vol. 61, No. 2, pp. 236–243. © Allerton Press, Inc., 2018.
Original Russian Text © A.M. Molchanov, A.S. Myakochin, 2018, published in Izvestiya Vysshikh Uchebnykh Zavedenii, Aviatsionnaya Tekhnika, 2018, No. 2, pp. 85–92.

AERO- AND GAS-DYNAMICS OF FLIGHT VEHICLES AND THEIR ENGINES

Numerical Simulation of High-Speed Flows Using the Algebraic Reynolds Stress Model

A. M. Molchanov[a, *] **and A. S. Myakochin**[a]

[a]*Moscow Aviation Institute (National Research University), Volokolamskoe sh. 4, Moscow, 125993 Russia*

**e-mail: heat204@mai.ru*

Received February 19, 2018

Abstract—A turbulence model for high-speed compressible flows is developed. It is based on modeling the rapid and slow parts of pressure-strain correlation depending on gradient Mach number and on the assumption that the velocity fluctuations normal to streamlines play a key role in turbulent mixing process. It is shown that an increase in the flow velocity leads to a slowing of turbulent mixing and an increase in the anisotropy of the flow. Comparison of the calculation results with the available experimental data showed good agreement.

DOI: 10.3103/S1068799818020125

Keywords: turbulence, supersonic flows, pressure-strain correlation, strain rate tensor.

Modeling of turbulence is extremely important in solving problems of airspace engineering [1]. It is well known that compressibility in high-speed flows has a stabilizing effect on turbulence so that the intensity of turbulent mixing reduces as velocity increases. This effect plays an important role in present-day problems of rocket and airspace engineering. For example, the rate of fuel and oxidizer mixing in supersonic engines is reduced. Compressibility changes the nature of laminar-turbulent boundary-layer transition over hypersonic vehicles during re-entry.

In most turbulence models used, the effect of high-speed compressibility was taken into account by adding additional dissipation to the turbulent kinetic energy (TKE) transport equation [2, 3]. However, in more recent works, for example, in [4], it was shown that this effect is manifested through the mechanism of interaction of pressure and velocity gradient rather than through dissipation.

In addition, the models based on supplementing additional dissipation to the equation of turbulent kinetic energy fail to predict the increasing turbulence anisotropy. The experiments [5, 6] showed that as the Mach number increases, the cross-stream turbulence fluctuations are affected in a greater extent than the streamwise ones.

The equations for the transport of the Reynolds stresses $R_{ij} = \widetilde{u_i'' u_j''}$ have the following form:

$$\frac{\partial}{\partial t}\left(\overline{\rho} R_{ij}\right) + \frac{\partial}{\partial x_k}\left(\overline{\rho}\tilde{u}_k R_{ij}\right) = T_{ij} + P_{ij} + \Pi_{ij} - \overline{\rho}\varepsilon_{ij}, \tag{1}$$

where T_{ij} is the turbulent, molecular and pressure-related diffusion; $P_{ij} = -\left(\overline{\rho u_i'' u_k''}\frac{\partial \widetilde{u_j}}{\partial x_k} + \overline{\rho u_j'' u_k''}\frac{\partial \widetilde{u_i}}{\partial x_k}\right)$ is the production of Reynolds stresses; ε_{ij} is the dissipative term that, taking into account local isotropy, is modeled as

$$\varepsilon_{ij} = \frac{2}{3}\varepsilon\delta_{ij}; \tag{2}$$

$\Pi_{ij} = \left(\overline{p' \frac{\partial u_i''}{\partial x_j}} + \overline{p' \frac{\partial u_j''}{\partial x_i}} \right)$ is the pressure–strain correlation. Here ε is the TKE dissipation rate.

The modeling of Π_{ij} depends on the flow rate, i.e. on the Mach number.

First, let us consider low speeds. Pressure–strain correlation is divided into the slow and rapid parts:

$$\Pi_{ij} = \Pi_{ij}^{(s)} + \Pi_{ij}^{(r)}. \tag{3}$$

For the slow part that characterizes the tendency towards isotropy, the following formula is used

$$\Pi_{ij}^{(s)} = -C_1 \overline{\rho} \varepsilon \left(\frac{R_{ij}}{K} - \frac{2}{3} \delta_{ij} \right), \tag{4}$$

for the rapid part a simplified model of Launder–Reece–Rodi [7] is used:

$$\Pi_{ij}^{(r)} = -\Gamma \left(P_{ij} - \frac{2}{3} P \delta_{ij} \right), \tag{5}$$

where P is the TKE production.

The numerical coefficients have the following meanings [7]:

$$C_1 = 1.5; \quad \Gamma = 0.6. \tag{6}$$

In the case of a compressible fluid, the tensor Π_{ij} ceases to be a divergence-free (that is, the trace of this tensor is not zero). Consequently, formulas (4) and (5) no longer reflect the correct nature of the pressure–strain interaction.

It is proposed in [8] to add an additional term proportional to the production P_{ij}: $-C_{\Pi 2}\left(M_G\right) P_{ij}$ to the formula (5).

In addition, it is shown that the coefficients C_1, Γ are no longer constants, but depend on the gradient Mach number that is defined as follows:

$$\mathrm{M}_G = \frac{S K^{3/2}}{a \varepsilon}, \quad S = \sqrt{2 S_{ij}^* S_{ij}^*}, \quad S_{ij}^* = S_{ij} - \frac{1}{3} \frac{\partial \tilde{u}_k}{\partial x_k} \delta_{ij}, \tag{7}$$

where a is the speed of sound.

In [8], on the basis of direct numerical simulation, formulas were obtained for all the coefficients that appear in the correction coefficients for the compressibility.

An analysis of these formulas shows that for a rapid part of Π_{ij} the correction coefficients for compressibility vary approximately equally depending on M_G, therefore, in this paper, a unified correction is proposed for this: $C_{\Pi 1}\left(\mathrm{M}_G\right)$.

Thus, for compressible flows, the following formula is proposed

$$\Pi_{ij} = -\hat{C}_1\left(\mathrm{M}_G\right) \overline{\rho} \varepsilon \left(\frac{R_{ij}}{K} - \frac{2}{3} \delta_{ij} \right) + C_{\Pi 1}\left(\mathrm{M}_G\right) \Pi_{ij}^{(r)} - C_{\Pi 2}\left(\mathrm{M}_G\right) P_{ij}, \tag{8}$$

where for the coefficients that take into account the compressibility, the following relations are used

$$\hat{C}_1 = C_1 \left[0.2786 \exp\left(-4,7758 \mathrm{M}_G^*\right) + 0.7213 \exp\left(-0.0334 \mathrm{M}_G^*\right) \right]; \tag{9}$$

$$C_{\Pi 1} = 0.9978 \exp\left(-2.2155 \mathrm{M}_G^*\right); \tag{10}$$

$$C_{\Pi 2} = \frac{17 \mathrm{M}_G^{*\,3}}{\left[\exp\left(8 \mathrm{M}_G^*\right) - 0.999 \right]}, \tag{11}$$

where $\mathrm{M}_G^* = \mathrm{M}_G / 3.05$.

For relations (9), (10), the approximation formulas from [8] are used, and relation (11) is obtained in this paper.

The dependence of the coefficients in the pressure-strain correlation on the gradient Mach number is shown in Fig. 1.

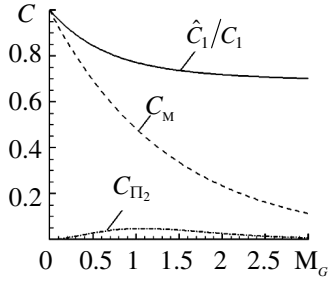

Fig. 1.

Thus, the source in the basic equation (1) is equal to

$$R_{ij} = \left(1 - C_{\Pi 2} - \hat{\Gamma}\right) P_{ij} - \hat{C}_1 \rho\varepsilon \frac{R_{ij}}{K} + \left[\left(\hat{C}_1 - 1\right)\rho\varepsilon + \hat{\Gamma} P\right]\frac{2}{3}\delta_{ij}, \quad \hat{\Gamma} = \Gamma C_{\Pi 1}. \tag{12}$$

Similar relationships can be easily obtained when using the Menter baseline (BSL) model [9].

A complete system of differential equations for transport of the Reynolds stresses is used in practice much less frequently than two-parameter models, such as k–ε or SST, because they do not give a significant improvement in the results of calculating turbulent flows, in addition they are much more complicated. Nevertheless, the analysis of these equations makes it possible to obtain important regularities for the determination of parameters entering into simpler models. In particular, this concerns the mechanism of affecting high-speed compressibility on turbulence.

For this analysis, we use a so-called algebraic stress model, which is based on the assumption of similarity of the transfer of Reynolds stresses and turbulent kinetic energy.

In this paper, we use the assumption of equilibrium of the convective and diffusion fluxes of turbulent stresses. It follows from this assumption that $R_{ij} = 0$, and that the trace of the tensor is also zero:

$$R_{kk} = \left(1 - C_{\Pi 2}\right) P_{kk} - 2\rho\varepsilon = 0; \quad 2P \equiv P_{kk} = \frac{2\rho\varepsilon}{\left(1 - C_{\Pi 2}\right)}. \tag{13}$$

Taking into account Eq. (12) and its analogue for BSL, we obtain the following algebraic formulas for the Reynolds stresses:

$$\frac{R_{ij}}{K} = \frac{\left(1 - C_{\Pi 2} - \Gamma C_{\Pi 1}\right) P_{ij}}{\hat{C}_1 \rho\varepsilon} + \frac{1}{\hat{C}_1}\left[\left(\hat{C}_1 - 1\right) + \frac{\Gamma C_{\Pi 1}}{\left(1 - C_{\Pi 2}\right)}\right]\frac{2}{3}\delta_{ij}; \tag{14}$$

$$\frac{R_{ij}}{K} = \frac{\left(1 - C_{\Pi 2}^* - \Gamma C_{\Pi 1}^*\right) P_{ij}}{\hat{C}_1 \overline{\rho}\beta'\omega K} + \frac{1}{\hat{C}_1}\left[\left(\hat{C}_1 - 1\right) + \frac{\Gamma C_{\Pi 1}^*}{\left(1 - C_{\Pi 2}^*\right)}\right]\frac{2}{3}\delta_{ij}, \tag{15}$$

where $C_{\Pi 1}^*, C_{\Pi 2}^*$ are formed using a transition function F_1 [9].

The obtained equations contribute little in comparison with the basic model of Reynolds stresses, since the solution of nonlinear algebraic systems of equations is not simpler than the solution of a system of partial differential equations.

Therefore, we use one more assumption. Let us consider streamlines introduced on the basis of Favre averaged velocities. It is reasonable to assume that the derivatives of the velocity along the streamlines will be substantially smaller than the derivatives along the normal to them

$$\frac{\partial}{\partial n} >> \frac{\partial}{\partial s} \text{ for } V_s, V_n, \tag{16}$$

and also that $V_s >> V_n$. Note that V_s, V_n are the instantaneous rather than averaged values of velocities, so V_n may not be equal to zero, in contrast to the average velocity $\tilde{V}_n \equiv 0$.

For a plane-parallel flow (*xy* plane) along the *x* axis, using assumption (16), we obtain rigorously:

$$P = -\rho\widetilde{u''v''}\frac{\partial u}{\partial y}; \quad P_{\widetilde{u''^2}} = -2\rho\widetilde{u''v''}\frac{\partial u}{\partial y} = 2P; \quad P_{\widetilde{v''^2}} = P_{\widetilde{w''^2}} = 0; \quad P_{\widetilde{u''v''}} = -\rho\widetilde{v''^2}\frac{\partial u}{\partial y}, \tag{17}$$

where *u*, *v*, *w* are the velocity components along the *x, y, z* axes.

Similar relationships are valid for arbitrary curvilinear streamlines:

$$P = -\overline{\rho}\widetilde{V_s''V_n''}\frac{\partial \tilde{V}_s}{\partial n}; \quad P_{\widetilde{V_s''^2}} = -2\overline{\rho}\widetilde{V_s''V_n''}\frac{\partial \tilde{V}_s}{\partial n} = 2P; \quad P_{\widetilde{V_n''^2}} = 0; \quad P_{\widetilde{V_s''V_n''}} = -\overline{\rho}\widetilde{V_n''^2}\frac{\partial \tilde{V}_s}{\partial n}. \tag{18}$$

From this, taking into account formulas (13) – (15), we obtain the explicit formulas for $\widetilde{V_n''^2}$ and $\widetilde{V_s''V_n''}$. In addition, testing the proposed model in the calculations and comparing it with the experimental data showed that a better agreement is obtained if the compressibility effect on the coefficients is not considered in the formulas for shear stress. Thus, the following formulas are obtained from the expressions (14), (15):

$$\frac{\widetilde{V_n''^2}}{K} = \frac{1}{\hat{C}_1}\left[\left(\hat{C}_1 - 1\right) + \frac{\Gamma C_{\Pi 1}}{\left(1 - C_{\Pi 2}\right)}\right]\frac{2}{3}, \quad \widetilde{V_s''V_n''} = -\frac{\left(1-\Gamma\right)}{C_1}\frac{\widetilde{V_n''^2}}{K}\frac{K^2}{\varepsilon}\frac{\partial \tilde{V}_s}{\partial n}; \tag{19}$$

$$\frac{\widetilde{V_n''^2}}{K} = \frac{1}{\hat{C}_1}\left[\left(\hat{C}_1 - 1\right) + \frac{\Gamma C^*_{\Pi 1}}{\left(1 - C^*_{\Pi 2}\right)}\right]\frac{2}{3}, \quad \widetilde{V_s''V_n''} = -\frac{\left(1-\Gamma\right)}{C_1\beta'}\frac{\widetilde{V_n''^2}}{K}\frac{K}{\omega}\frac{\partial \tilde{V}_s}{\partial n}. \tag{20}$$

Let us compare expressions (19) and (20) with formulas for turbulent shear stresses using models based on the concept of turbulent viscosity.

The standard *k*–ε model is

$$\overline{\rho}\widetilde{V_s''V_n''} = -\mu_T\frac{\partial \tilde{V}_s}{\partial n}; \quad \mu_T = 0.09\overline{\rho}\frac{K^2}{\varepsilon}. \tag{21}$$

Standard model SST is

$$\overline{\rho}\widetilde{V_s''V_n''} = -\mu_T\frac{\partial \tilde{V}_s}{\partial n}; \quad \mu_T = \min\left(\frac{\overline{\rho}K}{\omega}, \frac{\overline{\rho}a_1K}{\Omega F_2}\right). \tag{22}$$

Such a comparison allows us to propose formulas for turbulent viscosity, in which it is possible to take into account the effect of high-speed compressibility via the coefficients $\hat{C}_1, C_{\Pi 1}, C_{\Pi 2}$:

$$\mu_T = 0.09\frac{C_\mu}{C_\mu(0)}\overline{\rho}\frac{K^2}{\varepsilon}, \quad C_\mu = \frac{\left(1-\Gamma\right)}{C_1}\frac{\widetilde{V_n''^2}}{K}; \tag{23}$$

$$\mu_T = \min\left(\frac{C_\mu}{C_\mu(0)}\overline{\rho}\frac{K}{\omega}, \frac{\overline{\rho}a_1K}{\Omega F_2}\right), \quad C_\mu = \frac{\left(1-\Gamma\right)}{C_1}\frac{\widetilde{V_n''^2}}{K}. \tag{24}$$

Here, $C_\mu(0)$ means the value of C_μ at low speeds: $\mathrm{M}_G \approx 0 \to C_{\Pi 1} = 1;\ C_{\Pi 2} = 0$. If we use the values $C_1 = 1.5,\ \Gamma = 0.6$, then $\widetilde{V_n''^2}/K = 0.49,\ C_\mu(0) = 0.13$, and if $C_1 = 1.8,\ \Gamma = 0.6$, then $\widetilde{V_n''^2}/K = 0.52$, $C_\mu = 0.115$.

By taking the trace of Eq. (1), we obtain the transport equation for turbulent kinetic energy:

$$\frac{\partial}{\partial t}\left(\overline{\rho}K\right)+\frac{\partial}{\partial x_k}\left(\overline{\rho}\tilde{u}_k K\right)=\frac{\partial}{\partial x_k}\left[\left(\mu+\mu_T\right)\frac{\partial K}{\partial x_k}\right]+\left(1-C_{\Pi 2}\right)P-\overline{\rho}\varepsilon\,; \tag{25}$$

$$\frac{\partial}{\partial t}\left(\overline{\rho}K\right)+\frac{\partial}{\partial x_j}\left(\overline{\rho}\tilde{u}_j K\right)=\frac{\partial}{\partial x_j}\left[\left(\mu+\frac{\mu_T}{\sigma_K}\right)\frac{\partial K}{\partial x_j}\right]+\left(1-C^*_{\Pi 2}\right)P-\overline{\rho}\beta'\omega K\,. \tag{26}$$

Testing the turbulence model considering the compressibility effect involved comparing the simulation results using this model with the available experimental data for various types of flow.

1. Mixing Layer.

This test involved the comparison with the experimental data of [5, 8]. A plane mixing of two parallel gas flows having different velocities and densities was investigated. The table presents the main parameters of these flows for seven options.

Flow parameters	Option						
	1	1d	2	3	3r	4	5
$r=U_2/U_1$	0.78	0.79	0.57	0.18	0.25	0.16	0.16
$s=\rho_2/\rho_1$	0.76	0.76	1.55	0.57	0.58	0.6	1.14
M_1, M_2	2.01; 1.38	2.02; 1.39	1.91; 1.36	1.96; 0.27	2.22; 0.43	2.35; 0.3	2.27; 0.38
$M_r=\Delta U/\overline{a}$	0.4	0.4	0.91	1.37	1.44	1.73	1.97
T_1, T_2, K	163; 214	151; 198	334; 215	161; 281	159; 275	171; 285	332; 292
U_1, U_2, m/s	515; 404	498; 392	700; 399	499; 92	561; 142	616; 100	830; 131
P, Pa	46e3	55e3	49e3	53e3	53e3	36e3	32e3

We represent the normalized similarity profiles of Reynolds stress $\tau_{uv}=\widetilde{u_1'' u_2''}$ (Fig. 2a) and the cross-stream turbulence intensity $\sigma_v=\sqrt{\widetilde{u_2''u_2''}}$ (Fig. 2b).

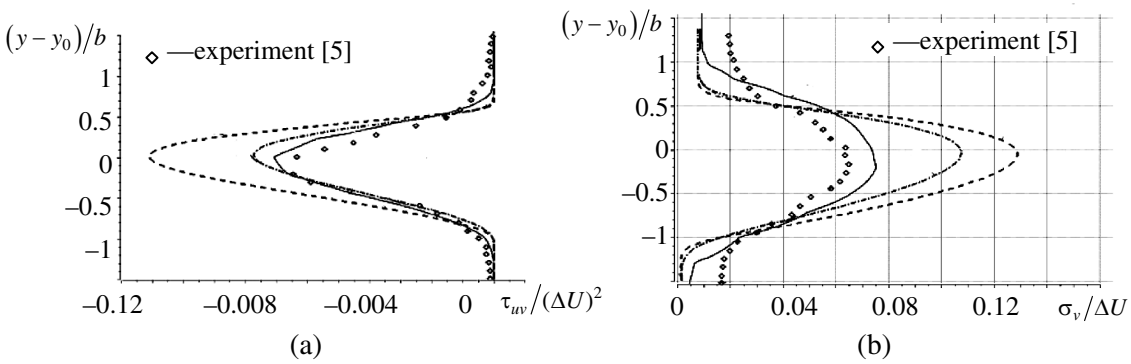

Fig. 2.

Figure 3 shows the normalized similarity profiles of streamwise turbulence intensity $\sigma_u=\sqrt{\widetilde{u_1''u''}_1}$. Here: $\Delta U=U_1-U_2$; b is the thickness of the mixing layer; y_0 is the transverse coordinate corresponding to the average velocity $0.5\left(U_1+U_2\right)$; $\sigma_u=\sqrt{\widetilde{u_1''u''}_1}$; $\sigma_v=\sqrt{\widetilde{u_2''u_2''}}$. The calculations were compared with the use of three models of turbulence: - - - —standard k–ε model; - ·-·- —k–ε model with compressibility corrections [3]; —— —the model presented in this paper.

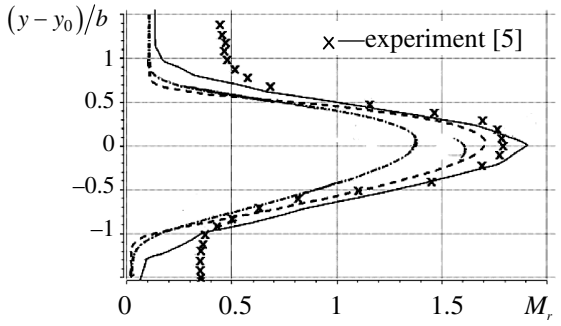

Fig. 3.

The best match is achieved when the model proposed in this paper is used.

Figure 4 shows the effect of the relative flow rate $M_r = (U_1 - U_2)/\bar{a}$ on the main turbulent mixing parameters: (a)—the expansion velocity of the mixing layer; (b)—the shear stress. The calculated parameters are normalized to their analogues, obtained without taking into account the compressibility effect in the model in turbulence at the same values of the ratio of the velocities $r = U_2/U_1$ and the ratio of densities $s = \rho_2/\rho_1$.

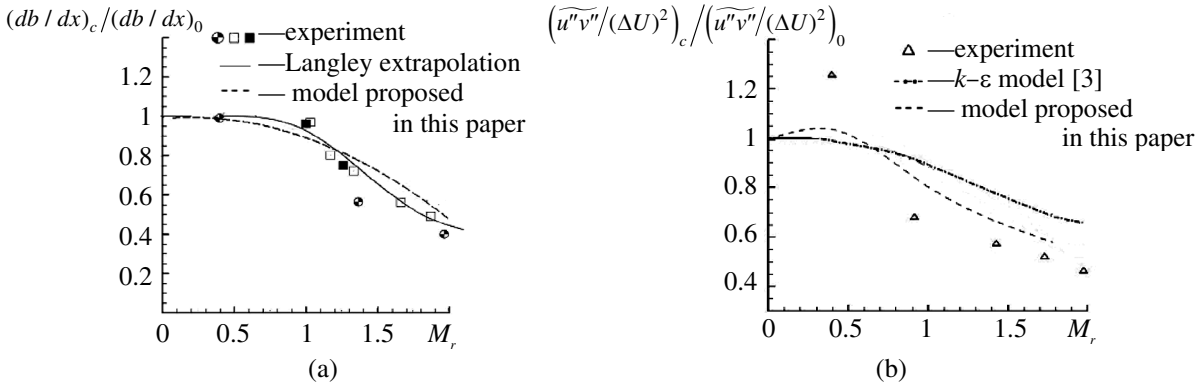

Fig. 4.

Figure 5 shows the dependence of the anisotropy of turbulence on the Mach number using different models of turbulence and comparison with experiment.

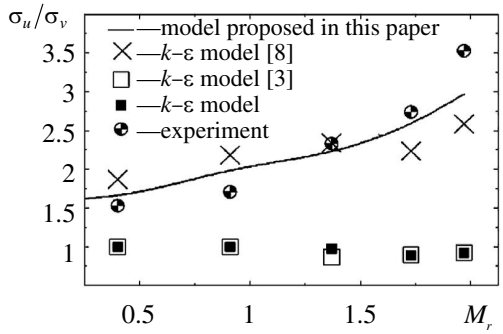

Fig. 5.

2. Fully Expanded Heated Free Jets.

This test was aimed at validating the turbulence model presented for the simulation of jets, temperature, density and pressure of which at the nozzle exit (indicated by the subscript *a*) are the same as those in the ambient (subscript *e*), i.e. $T_a = T_e, \rho_a = \rho_e, p_a = p_e$.

This condition makes an estimate of a pure effect of compressibility on jet parameters. Simulations with *k*–ε model, Sarkar's *k*–ε cc model [3] and model proposed in this paper were performed and compared.

The results of the simulation were compared with the experimental data [10, 11].

It is rather difficult to determine experimentally the length of the initial section of the jet with sufficient accuracy. To estimate the jet length, it is more convenient to use a dimensionless coordinate $\overline{X}_{0.75} = X_{0.75}/R_a$ from the nozzle exit corresponding to the value of the relative velocity $u_C/u_a = 0.75$ [10, 11]. It should be noted that, in accordance with the data of [11], the maximum intensity of turbulence and the velocity gradient is observed precisely in the cross section $\overline{X}_{0.75}$.

Figure 6 shows the dependence of the relative coordinate $\overline{X}_{0.75}$ on the Mach number at the nozzle exit. The simulation results were compared with the experimental data [10, 11].

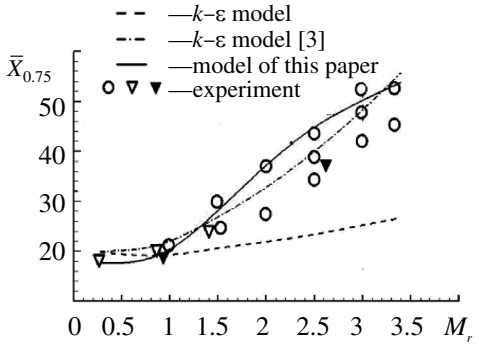

Fig. 6.

3. Under-Expanded Cold Supersonic Air Jet.

Results of calculation of an under-expanded supersonic jet and comparison with experimental data are presented [12]. The simulation was carried out for jets having a total temperature $T_0 = 300\,\mathrm{K}$ and the output Mach number $\mathrm{M}_a = 3.3$.

Figure 7 presents the simulation results and the experimental data for an under-expanded jet with static pressure ratio $p_a/p_e = 1.5$, diameter of the profiled nozzle $D_a = 53.7$ mm and nozzle exit half cone angle $\theta_a = 10$ deg.

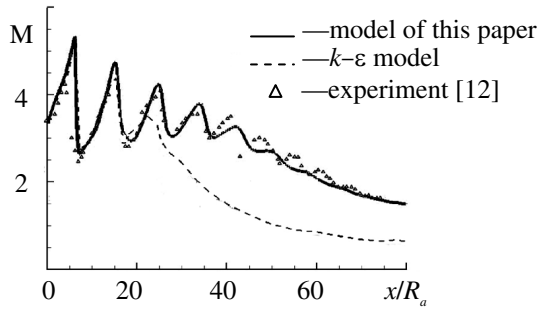

Fig. 7.

Using standard k–ε model considerably under-predicts the jet length if compared with the experimental data, and also reduces a number of shock diamonds in the jet. The oscillations of the Mach number have much lower amplitude than in the experiment.

An analysis of the results obtained showed that the turbulent mixing decreases as the velocity increases. An increase in the relative velocity leads to a decrease in the shear stress, a significant decrease in the transverse velocity pulsations, and a very slight change in the longitudinal pulsations. This means that the compressibility affects the velocity fluctuations directed normally to the streamlines, first of all, and through this value it affects the shear stress. The effect of compressibility on velocity fluctuations along the streamlines is small.

REFERENCES

1. Mingazov, B.G. and Davletshin, I.S., On Choice of Turbulence Models and Grid Parameters for Computation of Flows in Diffuser Ducts, *Izv. Vuz. Av. Tekhnika,* 2011, vol. 54, no.4, pp. 24–28 [Russian Aeronautics (Engl. Transl.), vol. 54, no. 4, pp. 359–366].
2. Glebov, G.A. and Molchanov, A.M., Model of Turbulence for Supersonic Reacting Jets, *Issledovanie teploobmena v letatelnykh apparatakh* (Investigation of Heat Transfer in Flying Vehicles), Moscow: MAI, 1982, pp. 6–11.
3. Sarkar, S., Erlebacher, G., and Hussaini, M.Y., Compressible Homogeneous Shear: Simulation and Modeling, *NASA Contractor Report 189611, ICASE Report no. 92-6 / NASA,* Washington, 1992.
4. Vreman, A.W., Sandham, N.D., and Luo, K.H., Compressible Mixing Layer Growth Rate and Turbulence Characteristics, *Journal of Fluid Mechanics*, 1996, vol. 320, pp. 235–258.
5. Goebel, S.G. and Dutton, J.C. Experimental Study of Compressible Turbulent Mixing Layers, *AIAA Journal*, 1991, vol. 29, no. 4, pp. 538–546.
6. Simone, A., Coleman, G.N., and Cambon, C., The Effect of Compressibility on Turbulent Shear Flow: a Rapid-Distortion-Theory and Direct-Numerical-Simulation Study, *Journal of Fluid Mechanics*, 1997, vol. 330, pp. 307–338.
7. Launder, B.E., Reece, G.J., and Rodi, W., Progress in the Developments of a Reynolds-Stress Turbulence Closure, *Journal of Fluid Mechanics*, 1975, vol. 68, no. 3, pp. 537–566.
8. Gomez, C.A. and Girimaji, S.S., Explicit Algebraic Reynolds Stress Model (EARSM) for Compressible Shear Flows, *Theoretical and Computational Fluid Dynamics*, 2014, vol. 28, no. 2, pp. 171–196.
9. Eisfeld, B., Rumsey, C., and Togiti, V., Verification and Validation of a Second-Moment-Closure Model, *AIAA Journal*, 2016, vol. 54, no. 5, pp. 1524–1541.
10. Lau, J.C., Morris, P.J., and Fisher, M.J., Measurements in Subsonic and Supersonic Free Jets Using a Laser Velocimeter, *Journal of Fluid Mechanics*, 1979, vol. 93, no. 1, pp. 1–27.
11. Krasotkin, V.S., Myshanov, A.I., Shalaev, S.P., Shirokov, N.N. and Yudelovich, M.Ya., Investigation of Supersonic Isobaric Submerged Turbulent Jets, *Izv. AN SSSR. Mekhanika Zhikosti i Gaza*, 1988, no. 4, pp. 56–62 [Fluid Dynamics, 1988, vol. 23, no. 4, pp. 529–534].
12. Safronov, A.V. and Khotulev, V.A., Results of Experimental Researches of the Supersonic Cold and Hot Jet, *Fiziko-Khimicheskaya Kinetika v Gazovoi Dinamike* [Electronic journal], 2008, vol. 6, URL: http://chemphys.edu.ru/issues/2008-6/articles/280/.